



## Influence of Carbon Nanotubes on Thermal Expansion Coefficient and Thermal Buckling of Polymer Composite Plates: Experimental and Numerical Investigations

Journal:	<i>Mechanics Based Design of Structures and Machines, An International Journal</i>
Manuscript ID	LMBD-2019-0174.R4
Manuscript Type:	Research Papers
Date Submitted by the Author:	25-Sep-2019
Complete List of Authors:	Kamarian, S.; Amirkabir University of Technology Bodaghi, Mahdi; Nottingham Trent University Barbaz, Reza; Amirkabir University of Technology Shakeri, Mahmoud; Amirkabir University of Technology Yas, M. H.; Razi University
Keywords:	Multi-Walled Carbon Nanotubes, Nanocomposites, Experiments, Coefficient of Thermal Expansion, Thermal Buckling

SCHOLARONE™  
Manuscripts

# Influence of Carbon Nanotubes on Thermal Expansion Coefficient and Thermal Buckling of Polymer Composite Plates: Experimental and Numerical Investigations

S. Kamarian<sup>a †</sup>, M. Bodaghi<sup>b</sup>, R. Barbaz Isfahani<sup>a</sup>, M. Shakeri<sup>a</sup>, M. H. Yas<sup>c</sup>

a. Department of Mechanical Engineering, Amirkabir University of Technology, Tehran, Iran

b. Department of Engineering, School of Science and Technology, Nottingham Trent University, Nottingham, NG11 8NS, United Kingdom

c. Department of Mechanical Engineering, Razi University, Kermanshah, Iran

---

† Corresponding Author, E-mail: [kamarian.saeed@yahoo.com](mailto:kamarian.saeed@yahoo.com)

## Abstract

The first aim of this paper is to experimentally explore the effect of multi-walled carbon nanotubes (MWCNTs) on the coefficient of thermal expansion (CTE) of epoxy-based composites. Focusing on the obtained experimental data, two important conclusions can be drawn. 1) Though the CTE of carbon nanotubes (CNTs) is lower than that of neat epoxy, using more CNT does not necessarily decrease the CTE of epoxy polymer. 2) The optimum weight percent of CNT is 0.3 which can reduce the CTE of epoxy up to 33%. As the second goal of the present research work, thermal buckling analysis of rectangular carbon fiber-reinforced CNT/epoxy polymer (CFRCNTEP) laminated composite plates is performed numerically. To this purpose, first, using the obtained experimental data and micro-mechanical models, the thermo-elastic properties of structure are calculated. Then, based on the first-order shear deformation theory (FSDT) and by means of generalized differential quadrature (GDQ) method, the influence of CNTs on the critical buckling temperature of CFRCNTEP composite plates is investigated. The numerical results reveal that MWCNTs can strongly affect thermal buckling behavior of composite plates. It is observed that by adding 0.3 wt% CNTs into the matrix phase, the critical buckling temperature increases between 35 to 42%.

**Keywords:** Multi-Walled Carbon Nanotubes, Nanocomposites, Experiments, Coefficient of Thermal Expansion, Thermal Buckling

## 1. Introduction

Polymeric resins are extensively used as matrices for structural composite materials due to their high stiffness, low creep, superior chemical resistance and excellent adhesion to fillers and fibers (Mallick 2007). The CTE of polymers is one of most important thermo-mechanical properties for designing polymer based composite structures when exposed to thermal environments. For instance, one of reasons for micro-crack phenomenon in fiber-reinforced polymers laminated composites during the temperature cycling is the difference of thermal properties like CTE between reinforcing fibers and resin. This matter becomes a serious problem for carbon fiber-reinforced epoxy polymer (CFREP) laminated composites because the CTEs of carbon fibers is about  $-12 \times 10^{-6} \text{ }^{\circ}\text{C}^{-1}$  while  $65 \times 10^{-6} \text{ }^{\circ}\text{C}^{-1}$  for epoxy resins, respectively. Thus, it is preferred having epoxy resins with low CTE when carbon fibers as reinforcing phase. The other importance of polymer's CTE becomes evident when thermal stresses in composite structures are concentrated. Generally, when a composite structure is heated, it usually tends to expand and experiences thermal stress. It can be shown that the thermal expansion and thermal stress are extremely dependent on the CTE (Reddy 2004). That is why, resins with low CTE are desired for composite structures when they are used under thermal environments. Another importance of CTE of resins is related to the thermal buckling in composite elements. This destructive phenomenon happens in thin composites when the structures with special boundary constraints and lamination scheme are exposed to thermal environments. Thermal buckling of composite structures is known as a failure mode and should be prevented in practice. To this end, many researchers have studied the effective parameters on thermal buckling of composite structures like stacking sequence of layers, geometrical parameters and boundary conditions. Using resins with low CTE can also help to decrease the compressive thermal stresses and delay the critical buckling temperature.

1  
2  
3 During last two decades, it has been shown that incorporation of nanomaterials such as CNTs can  
4 effectively improve thermo-mechanical properties of polymeric resin systems (Amir, BabaAkbar-  
5 Zarei and Khorasani 2019, Ayatollahi and Barbaz Isfahani 2017, Garg, Nam et al. 2019, Rafiee  
6 Zarei and Khorasani 2019, Ayatollahi and Barbaz Isfahani 2017, Garg, Nam et al. 2019, Rafiee  
7 2013, Rodríguez-González and Rubio-González 2019, Şansveren and Yaman 2019, Schadler,  
8 Giannaris, and Ajayan 1998, Sharma, and Mehta 2015, Siddiqui et al. 2009, Yazdi, 2019).  
9  
10 However, many researchers have shown that, increasing weight percent of CNTs does not  
11 necessarily increase the mechanical properties of composites in a monotonically increasing manner.  
12 The challenge in incorporating CNTs into polymers arises from several perspectives. Because of  
13 CNT's high aspect ratio, CNTs are capable of entanglements and as a consequence they will be  
14 expected to give very high increases in the system viscosity as the individual nanotubes un-bundle,  
15 one from the other. A second consideration is that the individual tubes are difficult to separate  
16 from each other as a result of Van der Waals forces that tend to make them clump together  
17 (Rahmandoust and Ayatollahi 2016). Also, when CNTs can be dispersed effectively, only at  
18 relatively low loading levels of 0.1 to 0.5 wt.% significant increase in mechanical properties of  
19 polymer matrices has been reported and by increasing the weight percent of loaded CNT, the  
20 properties decreased. The same trend was reported by previous studies as well (Maghsoudlou et  
21 al. 2019, Monfared, Ayatollahi and Isfahani 2018, Pötschke et al. 2003, Ren et al. 2003). Zhu *et*  
22 *al.* (2004) showed that increasing wt.% of CNTs does not always enhance all mechanical  
23 properties of composites. Manchado *et al.* (2005) concluded that increasing volume fraction of  
24 CNTs does not increase composite mechanical properties in a monotonically increasing manner.  
25 Barai and Weng (2011) experimentally and numerically showed that CNT agglomeration and  
26 imperfect interface condition can seriously reduce the effective stiffness and elasto-plastic strength.  
27 Rahman et al. (2012 b) investigated the influence of amino functionalized MWCNTs on thermo-

1  
2  
3 mechanical properties of e-glass/epoxy composites. They concluded that MWCNTs incorporation  
4 at low concentration (0.3 wt% as optimum loading) improves thermal and mechanical properties  
5 of e-glass/epoxy laminated composites. They also showed that using only 0.3 wt.% loading of  
6 MWCNTs increases the strength, Young's modulus and strain to failure of e-glass/epoxy  
7 composite up to 37%, 21% and 21%, respectively. It was also concluded from dynamic mechanical  
8 thermal analysis that the storage modulus, loss modulus and glass transition temperature ( $T_g$ ) of e-  
9 glass/epoxy composites increase 41%, 52% and  $10^\circ\text{C}$ , respectively when 0.3 wt% CNT was added  
10 to the epoxy resin. Anas *et al.* (2014) experimentally examined the effects of MWCNTs – as  
11 secondary reinforcements – on tensile strength, fiber-matrix bonding and interaction with the  
12 coupling agent in glass fiber/epoxy composites. From the experiments, it was observed that by  
13 using only 0.3 wt% CNTs, the tensile strength of the epoxy resin increases about 27%.  
14  
15  
16  
17  
18  
19  
20  
21  
22  
23  
24  
25  
26  
27  
28  
29

30 As can be found from the literature survey, although worthwhile researches have been dedicated  
31 to analyze the effect of MWCNTs on mechanical characteristics of epoxy polymers, to the best of  
32 the authors' knowledge, there are few research works on the influence of nanotubes on polymer's  
33 CTE (Ansari, Hassanzadeh-Aghdam and Darvizeh 2016, Dos Santos *et al.* 2008, Hameed *et al.*  
34 2015, He *et al.* 2018, Kundalwal and Meguid 2015, Rahman *et al.* 2012, Salam *et al.* 2013, Sharma  
35 and Sharma 2016, Shirasu *et al.* 2017, Shirasu *et al.* 2015). Among those available, Santos *et al.*  
36 (2008) experimentally investigated the CTE of MWCNT/Epoxy composites. They considered only  
37 two types of nanocomposites with 0.1 wt% and 0.5 wt% CNTs and compared the result with the  
38 neat epoxy. The experiments revealed that the nanocomposite with less CNTs (0.1 wt%) reduce  
39 the CTE of epoxy before and after  $T_g$ . On the other hand, it was found that, although nanocomposite  
40 with more CNTs does not have any effect on the CTE of epoxy when temperature is less than  $T_g$ ,  
41  
42  
43  
44  
45  
46  
47  
48  
49  
50  
51  
52  
53  
54  
55  
56  
57  
58  
59  
60

1  
2  
3 it increases the CTE after  $T_g$ . Rahman *et al.* (2012 a) investigated the effects of incorporating a  
4 uniformly dispersed 0.3 wt.% loading of MWCNTs into the pristine and polyol-toughened epoxy.  
5  
6 They found that adding 0.3 wt.% MWCNTs could increase the stiffness of the composite and  
7  
8 reduce CTE values of epoxy-based resins. Recently, He *et al.* (2018) used MWCNTs  
9  
10 functionalized with  $Fe_3O_4$  to improve thermo-mechanical properties of epoxy polymers. Their  
11  
12 experimental results indicated that  $Fe_3O_4$ /O-MWCNTs can increase the tensile strength, impact  
13  
14 strength of epoxy resin and micro-cracks resistance at cryogenic temperature of carbon fiber  
15  
16 reinforced epoxy polymer (CFREP) composites and decrease the CTEs of the epoxy resin.  
17  
18  
19  
20  
21

22  
23 Investigation of thermo-mechanical behavior of composite structures like beams, plates and shells  
24  
25 reinforced with CNTs has gained considerable attention in the recent years. Many research works  
26  
27 have been devoted to thermal behavior analysis of CNT-based composite structures (Ansari,  
28  
29 Torabi and Shojaei 2017, Arefi and Soltan Arani 2018, Farzam and Hassani 2018, Kiani 2017,  
30  
31 Sankar 2017, Shen 2012, Torabi, Ansari and Hassani 2019, Tung 2017). They mostly implemented  
32  
33 micro-mechanical models to predict thermo-mechanical properties of CNT/polymer composites.  
34  
35 However, these models always estimate composite material properties with an increasing trend  
36  
37 versus CNTs. As it has been observed experimentally and stated above, increasing wt.% of CNTs  
38  
39 does not always enhance thermo-mechanical properties of the composites monotonically and  
40  
41 further studies need to be conducted to clarify the matter.  
42  
43  
44  
45

46  
47 The prime objective of the present work is exploring the effects of MWCNTs loading on thermal  
48  
49 properties of nanocomposites in a board range of wt.%. Nanocomposites with LY-5052 epoxy  
50  
51 matrix and different wt.% loading of MWCNTs (0, 0.1, 0.3, 0.5, 0.7, 1) are fabricated. The  
52  
53 dispersion of the MWCNTs in the epoxy resin is made by ultrasound and high-speed shearing  
54  
55 techniques. A detailed experimental analysis of influence of loading of MWCNTs into the epoxy  
56  
57

1  
2  
3 resin on the CTE is carried out. Then, as for the second purpose, this research work aims at thermal  
4 stability analysis of rectangular CNTCF laminated plates. The main purpose is to investigate the  
5 influence of CNTs on thermal buckling of rectangular CFREP laminated composite plates. To this  
6 end, using the experimental data and micro-mechanical models, the thermo-elastic properties of  
7 hybrid CFRCNTEP composite plates are predicted. After the estimation of thermo-elastic features,  
8 based on the FSDT and using GDQ approach which has been successfully applied for analysis of  
9 composite structures (Golchi, Talebitooti and Talebitooti 2019, Shahedi and Mohammadimehr  
10 2019, Zarezadeh, Hosseini and Hadi 2019), the effect of adding CNTs into the epoxy resin on  
11 critical buckling temperature of structure with respect to the geometrical parameters, stacking  
12 sequence of layers and boundary conditions are comprehensively studied. Due to the absence of  
13 similar results in the specialized literature, this paper is likely to fill a gap in the-state-of-the-art of  
14 MWCNT/epoxy and CFRCNTEP composites.  
15  
16  
17  
18  
19  
20  
21  
22  
23  
24  
25  
26  
27  
28  
29  
30  
31  
32  
33

## 34 **2. Materials and Structures**

### 35 **2.1. Materials**

36  
37 Epoxy-based resins are widely used as matrix for composite materials. In this research work, the  
38 low-viscosity commercially available Araldite LY-5052 epoxy and Aradur HY-5052 hardener  
39 both purchased from Huntsman Corporation were used. This low viscosity epoxy makes the  
40 dispersion of additives and fabrication of composite specimens easier at the room temperature.  
41 MWCNTs used in this work were produced by the US Research nanomaterials. They are  
42 characterized by purity >95%, outer diameter: 20-30 nm, inner diameter: 5-10nm, tube length range:  
43 10-30 um, specific surface area >110m<sup>2</sup>/gr, and density: 2100 Kg/m<sup>3</sup>.  
44  
45  
46  
47  
48  
49  
50  
51  
52  
53  
54  
55  
56  
57  
58  
59  
60



## 2.2. Sample preparation

The polymer-matrix nanocomposites were prepared by ultrasound method as the simplest and most convenient high-power dispersion approach. Five types of nanocomposites containing 0, 0.1, 0.3, 0.5, 0.7 and 1 wt.% of MWCNTs were prepared separately as shown in Fig. 1 and described below:

First, the desired amounts of MWCNTs were weighed and mixed with the required amount of epoxy and stirred for 10 min at 500 rpm (Steps 1-2). The mixtures containing 0.1, 0.3, 0.5, 0.7 or 1 wt.% of MWCNTs were then sonicated for 50-70 min by a conventional ultrasonic (Step 3). During the sonication, the mixture container was held in iced water to keep the temperature around room temperature. In order to make sure the sonication energy was transferred uniformly to the whole mixture, the mixture was stirred every 5 min by a small spoon. Finally, to remove any bubble, the produced mixture was degassed in vacuum oven at room temperature for 15 min (Step 4). Six types of polymeric specimens (pure and nanocomposites) were initially fabricated by casting into the molds (considering sample dimensions characterized by the ASTM E831 standard) and curing for 24 h at room temperature, 25 °C (Step 5). The samples were then removed from the molds and post-cured for 1 h at 100 °C. Finally, the different types of samples were prepared to be investigated by TMA (Step 6).

## 2.3. Thermo-mechanical properties of nanocomposites polymer

Here, the approach by which thermo-mechanical properties epoxy/polymer matrix were calculated is described.

CTE of polymer matrix:

To obtain the CTE of the polymer matrix (pure epoxy and CNT/epoxy), thermo-mechanical analysis (TMA) was performed using TMA 500 device. In order to examine the accuracy of the analysis, first, the mean value of CTE was measured for pure epoxy ranging 20–100°C. Based on the obtained data from the experiment, the CTE for the pure polymer was found to be  $66 \times 10^{-6} / ^\circ\text{C}$ . It was compared with data sheet from the manufacturer listed in Table 1. A good agreement was observed between the results verifying accuracy of the fabrication procedure. Thus, the data of TMA test are accurate and acceptable for this research work.

In the next step, the CTE for nanocomposite polymer matrix containing 0, 0.1, 0.3, 0.5, 0.7 and 1 wt.% of MWCNTs was measured and represented in Fig. 2 and Table 2. The preliminary conclusion drawn from this figure is the fact that CTE has a decreasing-increasing trend against adding MWCNTs. In fact, the dependency of thermal properties of polymer matrix on wt.% of MWCNTs is not monotonic. As it can be seen, increasing wt.% of MWCNTs up to 0.3 reduces the CTE, while further increase has a negative effect and enhances the CTE. This phenomenon can be related to MWCNT agglomeration that dramatically influences CTE. To investigate the state of MWCNTs dispersion, three samples of the nanocomposite specimens with 0.3, 0.5 and 1 wt. % of MWCNTs are comparatively studied using transmission electron microscopy (TEM) as shown in Fig. 3. This figure illustrates the state of dispersion of fillers with different loadings. According to Fig. 3- a, a good dispersion of MWCNTs is observed for the specimen containing 0.3 wt. % of MWCNTs while some local MWCNT agglomerations are observed for the specimens with 0.5

1  
2  
3 and 1 wt. % of MWCNTs as shown in Figs. 3 b and c. Therefore, it can be concluded that the  
4  
5 optimum amount of nanotubes in order to decrease the CTE of polymers is 0.3 wt%. Similar results  
6  
7 have also been reported by other researchers for mechanical properties of nanocomposite polymers  
8  
9 that proves the fact that at an optimum amount of wt% of CNTs, some material properties like  
10  
11 Young's modulus sharply changes (Manchado et al. 2005).  
12  
13

14  
15 The results presented in Fig. 2 reveal that nanocomposite with 0.3 wt.% of MWCNTs has  
16  
17 minimum CTE of  $44 \times 10^{-6} / ^\circ\text{C}$  that is 33% smaller than its value for the pure polymer. Since the  
18  
19 main scope of the present work is related to the thermal buckling behavior of nanocomposite  
20  
21 structures, 0.3 wt.% of MWCNTs is considered as optimum amount of nanotubes. Fig. 2 also  
22  
23 illustrates that the CTE of CNT reinforced polymer cannot be calculated using rule-of-mixture  
24  
25 applied in many previous researches. According to this rule, the CTE of nanocomposite is always  
26  
27 decreased by increasing wt.% of MWCNTs. However, this is in contrast with experimental  
28  
29 observations in the present research work. It should be mentioned that the rule of mixture is not  
30  
31 also valid for composites with short fibers. Furthermore, it is not able to consider the agglomeration  
32  
33 effect of CNTs.  
34  
35  
36  
37  
38  
39

#### 40 Mechanical properties of epoxy/polymer matrix:

41  
42 The dependency of Young's modulus of the polymer-based composites on the low wt.% of  
43  
44 MWCNTs can be estimated by various micro-mechanical methods. Qian et al. (2000) showed that  
45  
46 if reinforcing MWCNTs bond strongly to the matrix, the external load is transmitted from the  
47  
48 matrix to MWCNTs via the interfacial shear stress. Considering MWCNTs as randomly oriented  
49  
50 discontinuous fiber lamina, Young's modulus of the nanocomposite,  $E_{NC}$ , can be calculated as  
51  
52 (Qian et al. 2000):  
53  
54  
55  
56  
57  
58  
59  
60

$$E_{NC} = \left[ \frac{3}{8} \frac{1 + 2(l_{NT} / d_{NT})\eta_L V_{NT}}{1 - \eta_L V_{NT}} + \frac{5}{8} \frac{1 + 2\eta_T V_{NT}}{1 - \eta_T V_{NT}} \right] E_P$$

$$\eta_L = \frac{(E_{NT} / E_P) - 1}{(E_{NT} / E_P) + 2(l_{NT} / d_{NT})} \quad (1)$$

$$\eta_T = \frac{(E_{NT} / E_P) - 1}{(E_{NT} / E_P) + 2}$$

where  $E_P$  and  $E_{NT}$  are Young's modulus of the polymer matrix and MWCNTs, respectively.  $l_{NT}$  and  $d_{NT}$  are the length and the outer diameter of the MWCNT, while  $V_{NT}$  denotes its volume fraction. Qian *et al.* (2000) used the above equation to calculate Young's modulus of polystyrene matrix reinforced by MWCNTs. They compared the experimental data with those obtained by the theoretical model of Eq. (1) and concluded that the mentioned model can predict the Young modulus of nanocomposite matrix with enough accuracy. Therefore, in this step, Eq. (1) is applied as an acceptable model to obtain the Young Modulus of MWCNT-reinforced polymer matrix. Using this solution, no experiment is needed to calculate the Young's modulus of nanocomposite polymer. Here, Young's modulus of the polymer is 3.1 *GPa* as reported by the manufacturer. Average values are considered for outer diameter and length of the MWCNT. Its Young's modulus is given by 0.2-0.8 TPa. Average Young's modulus is calculated by Eq. (1) for 0.3 wt.% of MWCNTs as 3.38 *GPa* that is 9% higher than pure polymeric one.

According to the data sheet from the manufacturer, the Poisson's ratio of the pure polymer is 0.35. Spanosa and Kontsos. (2008) showed that CNTs don't affect the Poisson's ratio of polymers by a considerable amount. Besides, for nanocomposite matrix and long carbon fibers, it is possible to use rule of mixture to calculate the Poisson's ratio of whole system. Thus, though the volume fraction of long carbon fibers in the present study is assumed to be 60%, the Poisson's ratio of hybrid composite system (CNT/Polymer/Carbon fibers) cannot change sharply. Therefore, the

Poisson's ratio of nanocomposite matrix with 0.3 wt.% of MWCNTs can be assumed to be 0.35.

A summary of the thermo-mechanical properties of pure polymer and nanocomposite with 0.3 wt.% of MWCNTs adopted from different methods is presented in Table 3.

#### 2.4. Thermo-mechanical properties of CFREP and CFRCNTEP composites

In the present work, long carbon fibers are assumed to reinforce pure epoxy and nanocomposites. Thermo-mechanical properties of carbon fibers are listed in Table 4 where  $E_1, E_2, G_{12}, \nu_{12}, \alpha_1, \alpha_2$  denote longitudinal and transverse Young's moduli, in-plane shear modulus, major Poisson's ratio, longitudinal and transverse thermal expansion coefficients, respectively. Having thermo-mechanical properties of pure epoxy, nanocomposite matrix and carbon fibers, material properties of CFREP and CFRCNTEP composites can be calculated from rule of mixture. The elastic properties of the long fiber-reinforced polymer composite are expressed as:

Young's modulus:

$$E_1 = E_1^f V^f + E^m V^m \quad (2)$$

$$\frac{1}{E_2} = \frac{\eta^f V^f}{E_2^f} + \frac{\eta^m V^m}{E^m}$$

$$\eta^f = \frac{E_1^f V^f + \left[ (1 - \nu_{12}^f \nu_{21}^f) E^m + \nu^m \nu_{21}^f E_1^f \right] V^m}{E_1^f V^f + E^m V^m}$$

$$\eta^m = \frac{E^m V^m + \left[ (1 - (\nu^m)^2) E_1^f - (1 - \nu^m \nu_{12}^f) E^m \right] V^f}{E_1^f V^f + E^m V^m}$$

Shear modulus:

$$\frac{1}{G_{12}} = \frac{V^f}{G_{12}^f} + \frac{V^m}{G^m} \quad (3)$$

$$\text{Thermal expansion coefficient: } \alpha_1 = \frac{\alpha_1^f E_1^f V^f + \alpha^m E^m V^m}{E_1^f V^f + E^m V^m} \quad (4)$$

$$\alpha_2 = \alpha_2^f V^f + \alpha^m V^m + \left( \frac{E_1^f \nu^m + E^m \nu_{12}^f}{E_1} \right) (\alpha^m - \alpha_1^f) (1 - V^f) V^f$$

$$\text{Poisson's ratio: } \nu_{12} = \nu_{12}^f V^f + \nu^m V^m \quad (5)$$

where subscripts 1 and 2 are related to the materials properties along the fiber direction and perpendicular to the fiber direction. Also, the superscripts 'm' and 'f' mean the matrix and carbon fiber, respectively. Considering material properties of pure epoxy, nanocomposite with 0.3 wt.% of MWCNTs and carbon fibers, the elastic properties of CFREP and CFRCNTep composites with  $V^f = 0.6$  are calculated and presented in Table 5. Comparing material properties of CFREP and CFRCNTep composite reveals that, MWCNTs result in minor and major improvements in mechanical and thermal properties of the composite. As it can be seen, adding up 0.3 wt.% of MWCNTs to the CFREP composite improves the CTE by 156.19% and 26.57% along the fiber direction and perpendicular to the fiber direction, respectively.

## 2.5. Governing equations

Consider a rectangular carbon-fiber/MWCNT/epoxy laminated composite plate as displayed in Fig. 4. The plate length is  $a$  and its width and total thickness are denoted by  $b$  and  $h$ , respectively. Orthogonal coordinate system namely  $(x, y, z)$  as shown in Fig. 4 is located on the middle surface of the composite plate.

Based on the FSDT, the governing equations for thermal buckling of symmetrically laminated plate are derived as (Reddy 2004):

$$D_{11} \left( \frac{\partial^2 \phi_x}{\partial x^2} \right) + D_{12} \left( \frac{\partial^2 \phi_y}{\partial x \partial y} \right) + D_{66} \left( \frac{\partial^2 \phi_x}{\partial y^2} + \frac{\partial^2 \phi_y}{\partial x \partial y} \right) - k_s A_{55} \left( \phi_x + \frac{\partial w}{\partial x} \right) - k_s A_{45} \left( \phi_y + \frac{\partial w}{\partial y} \right) + 2D_{16} \frac{\partial^2 \phi_x}{\partial x \partial y} + D_{16} \frac{\partial^2 \phi_y}{\partial x^2} + D_{26} \frac{\partial^2 \phi_y}{\partial y^2} = 0 \quad (6)$$

$$D_{66} \left( \frac{\partial^2 \phi_y}{\partial x^2} + \frac{\partial^2 \phi_x}{\partial x \partial y} \right) + D_{12} \left( \frac{\partial^2 \phi_x}{\partial x \partial y} \right) + D_{22} \left( \frac{\partial^2 \phi_y}{\partial y^2} \right) - k_s A_{44} \left( \phi_y + \frac{\partial w}{\partial y} \right) - k_s A_{45} \left( \phi_x + \frac{\partial w}{\partial x} \right) + D_{16} \frac{\partial^2 \phi_x}{\partial x^2} + D_{26} \frac{\partial^2 \phi_x}{\partial y^2} + 2D_{26} \frac{\partial^2 \phi_y}{\partial x \partial y} = 0 \quad (7)$$

$$k_s A_{55} \left( \frac{\partial \phi_x}{\partial x} + \frac{\partial^2 w}{\partial x^2} \right) + k_s A_{44} \left( \frac{\partial \phi_y}{\partial y} + \frac{\partial^2 w}{\partial y^2} \right) + k_s A_{45} \left( \frac{\partial \phi_x}{\partial y} + \frac{\partial \phi_y}{\partial x} + 2 \frac{\partial^2 w}{\partial x \partial y} \right) - N_x^T \frac{\partial^2 w}{\partial x^2} - 2N_{xy}^T \frac{\partial^2 w}{\partial x \partial y} - N_y^T \frac{\partial^2 w}{\partial y^2} = 0 \quad (8)$$

in which  $w$ ,  $\phi_x$  and  $\phi_y$  denote transverse deflection of the middle surface, and the rotations of the middle surface of the plate about  $y$  and  $x$  axes, respectively. In addition,  $k_s$  represents the shear correction factor,  $A_{ij}$  and  $D_{ij}$  are the transformed stretching stiffness and bending stiffness coefficient, respectively, and  $N_x^T$ ,  $N_y^T$  and  $N_{xy}^T$  are thermal force resultants (Reddy 2004). In the present work, simply supported and clamped boundary conditions are considered for the structure. For simplicity and convenience, the letters  $S$  and  $C$  are utilized to signify a simply supported edge and a clamped edge, respectively. For instance,  $SCSC$  denotes a plate which is simply supported at  $x=0, a$  and is clamped at  $y=0, b$ . Boundary conditions for  $SSSS$ ,  $SCSC$  and  $CCCC$  plates are considered as:

SSSS :

$$W = 0 ; \varphi_y = 0 ; D_{11} \frac{\partial \varphi_x}{\partial x} + D_{12} \frac{\partial \varphi_y}{\partial y} + D_{16} \left( \frac{\partial \varphi_x}{\partial y} + \frac{\partial \varphi_y}{\partial x} \right) = 0 , \text{ at } x = 0, a$$

$$W = 0 ; \varphi_x = 0 ; D_{12} \frac{\partial \varphi_x}{\partial x} + D_{22} \frac{\partial \varphi_y}{\partial y} + D_{26} \left( \frac{\partial \varphi_x}{\partial y} + \frac{\partial \varphi_y}{\partial x} \right) = 0 , \text{ at } y = 0, b$$

SCSC :

$$W = 0 ; \varphi_y = 0 ; D_{11} \frac{\partial \varphi_x}{\partial x} + D_{12} \frac{\partial \varphi_y}{\partial y} + D_{16} \left( \frac{\partial \varphi_x}{\partial y} + \frac{\partial \varphi_y}{\partial x} \right) = 0 , \text{ at } x = 0, a$$

$$W = 0 ; \varphi_x = 0 ; \varphi_y = 0 , \text{ at } y = 0, b$$

CCCC :

$$W = 0 ; \varphi_x = 0 ; \varphi_y = 0 , \text{ at } x = 0, a ; y = 0, b$$

Here, GDQ method as a powerful technique is employed to solve the governing equations (6)-(8) and obtain the buckling temperature of the structure. Based on the proposed method, the  $n$ th order of a continuous function  $f(\zeta)$  with respect to  $\zeta$  at a given point  $\zeta_i$  can be approximated as a linear sum of weighting values at all of the discrete point in the domain of  $\zeta$  (Bellman and Casti 1971, Shu and Richards, 1992),

$$\frac{\partial f^{n(\zeta_i)}}{\partial \zeta^n} = \sum_{j=1}^{N_\zeta} c_{ij}^n f(\zeta_j) , (i = 1, 2, N_\zeta , n = 1, 2, \dots, N_\zeta - 1) \quad (9)$$

where  $N_\zeta$  is the number of sampling points, and  $c_{ij}^n$  is the  $\zeta_j$  dependent weight coefficient.

### 3. Thermal buckling study

In this section, first, convergence and comparison studies are conducted to check the accuracy of the present solution. Afterward, parametric studies are performed to investigate the influences of geometric and material parameters on the thermal buckling behaviour of carbon-fibre-reinforced nanocomposite rectangular plates.



### 3.1. Convergence and comparison study

In order to validate the present formulation and solution methodology, critical buckling temperatures of rectangular CFREP laminated plates are predicted and compared with those reported in the literature. The present GDQ method with  $7 \times 7$ ,  $9 \times 9$ ,  $13 \times 13$  and  $17 \times 17$  grid points is implanted to compute critical buckling temperature parameter ( $\lambda_T = \alpha_0 \Delta T_{cr}$ ) of  $[0^\circ / 90^\circ]_s$  CFREP plates with *SSSS* and *CCCC* boundary conditions. The geometrical dimensions are  $a/b = 1$  and  $h/b = 0.01$ , and the material properties are as follows (Kant and Babu 2000):

$$\frac{E_1}{E_2} = 15, E_2 = E_3, \frac{G_{12}}{E_2} = \frac{G_{13}}{E_2} = 0.5, \frac{G_{23}}{E_2} = 0.3356, \nu_{12} = \nu_{13} = 0.3,$$

$$\frac{\alpha_1}{\alpha_0} = 0.015, \frac{\alpha_2}{\alpha_0} = \frac{\alpha_3}{\alpha_0} = 1, \alpha_0 = 10^{-6} 1/^\circ C$$

The results are presented in Table 6 and compared with their counterparts reported by Kant and Babu (2000). As it is evident, the results are so close to each other. Hence, it is concluded that GDQ can predict buckling temperatures of composite structures with high accuracy.

### 3.2. Parametric studies

In this section, thermal buckling behaviours of carbon-fibre-reinforced MWCNT/epoxy-based composite laminated rectangular plates are investigated. As experimentally observed in Fig. 2, the nanocomposite with 0.3 wt.% of MWCNTs has the minimum CTE of  $44 \times 10^{-6} 1/^\circ C^{-1}$  and therefore is considered as nanocomposite matrix in this section. The influence of MWCNTs on the thermal buckling of the composite rectangular plate with lamination scheme of  $[30^\circ / -45^\circ / 90^\circ]_s$  and length-to-width ratio of unity ( $a/b = 1$ ) is examined in Table 7. Critical buckling temperature difference is presented for composite plates with pure epoxy and MWCNT/epoxy matrices and

1  
2  
3 different thickness-to-length ratio,  $h/b$ . As expected, with the increase of thickness of plate the  
4 critical buckling temperature severely increases. Inspecting data given in Table 7 and Fig. 5, one  
5 can conclude that adding MWCNTs always enhances thermal buckling stability of the structure  
6 with various thicknesses. It has the same effect on the thermal buckling behaviour of plate with  
7 different thickness plates. It is observed that the critical buckling temperature of structure is  
8 improved around 37-39% for all plates.  
9

10  
11 In Table 8, the role of MWCNTs in variations of thermal buckling characteristics of a  
12  $[30^0 / -45^0 / 90^0]_s$  laminated plate with geometric parameters of  $a/b = 1$ ,  $h/b = 0.01$  for different  
13 types of boundary conditions is examined. It is obvious that the minimum, moderate and maximum  
14 values of  $\Delta T_{cr}$  correspond to *SSSS*, *SCSC* and *CCCC* cases, respectively. In fact, more constraints  
15 at the end edges enhance the structural stiffness resulting in a higher critical buckling temperature.  
16 It is also found that adding CNT into polymer matrix increases the critical buckling temperature  
17 of structure and this improvement is almost the same (37-39 %) for various types of boundary  
18 conditions.  
19

20  
21 Here, the influence of CNTs on the buckling temperature of laminated composite plates is  
22 investigated with respect to the carbon fiber angle. To this end, a square plate with angle-ply  
23 lamination scheme of  $[\theta / -\theta]_s$  is considered. The critical buckling temperature of the plate is  
24 calculated for various fiber angle  $\theta$  which can vary between  $-90^\circ$  and  $90^\circ$ , and the results are  
25 depicted in Fig. 6. This figure reveals that CNTs always have a positive effect on the thermal  
26 buckling stability of the plate with different lamination schemes ( $-90^\circ \leq \theta \leq 90^\circ$ ) and can enhance  
27 the critical buckling temperature of considered plate between 35% to 38.5%.  
28  
29  
30  
31  
32  
33  
34  
35  
36  
37  
38  
39  
40  
41  
42  
43  
44  
45  
46  
47  
48  
49  
50  
51  
52  
53  
54  
55  
56  
57  
58  
59  
60

1  
2  
3 In previous figures and tables, only the square type of plates was considered. The numerical results  
4 clarified that the CNTs are able to improve the buckling temperature of square laminated plates  
5 from 35 up to 38.5% for different  $h/b$  ratios, various lamination scheme and all types of boundary  
6 conditions. Now, the role of CNTs in variations of thermal buckling behavior of rectangular plates  
7 is examined. For this purpose, a diagram is presented to show the variations of buckling  
8 temperature against length-to-width parameter. Fig. 7 illustrate that CNTs always play a positive  
9 role in thermal buckling of composite plates with different  $a/b$  ratios. From Fig. 8, it is also  
10 concluded that with increase of  $a/b$  ratio, the CNTs become more effective at improving the  
11 stability of structure. In other words, the long plates are more affected by CNTs in comparison  
12 with square ones. The numerical results of Fig. 8 show that the thermal buckling characteristic of  
13 rectangular plates can be improved up to 42%.

## 31 32 **Conclusion**

33  
34  
35 The present research was dedicated to analyse and predict thermal properties of MWCNT/epoxy  
36 composites as well as thermal stability of carbon-fiber-reinforced MWCNT/epoxy composite  
37 laminated plates. Nanocomposites with epoxy matrix and different wt.% of MWCNTs (0, 0.1, 0.3,  
38 0.5, 0.7, 1) were made by ultrasound and high-speed shearing techniques. Thermal expansion  
39 coefficient of MWCNT/epoxy composites were measured and the effects of incorporating  
40 MWCNTs in the epoxy matrix were studied. Experimental results revealed that the CTE has a  
41 decreasing-increasing trend against adding up MWCNTs and becomes minimum for 0.3 wt.% of  
42 MWCNTs. Rule of mixture model were then implemented to calculate thermo-mechanical  
43 properties of carbon-fiber-reinforced MWCNT/epoxy composites. Then, thermal stability of  
44  
45  
46  
47  
48  
49  
50  
51  
52  
53  
54  
55  
56  
57  
58  
59  
60

1  
2  
3 rectangular laminated composite plates made of carbon-fiber-reinforced MWCNT/epoxy  
4  
5 composite laminae with low thermal expansion was investigated numerically. Based on FSDT and  
6  
7 by using GDQ approach, a parametric study was performed to demonstrate the effects of MWCNT  
8  
9 on thermal buckling of laminated rectangular plates. It was found that MWCNT is a highly  
10  
11 promising reinforcement for carbon-fiber-reinforced composite structures in thermal environments.  
12  
13 Results clarified that adding 0.3 wt.% of MWCNTs can improve critical buckling temperature  
14  
15 around 35-42 % for different thicknesses-to-width and length-to-width ratios, various stacking  
16  
17 sequences of layers and all types of boundary conditions. The benchmark results provided in this  
18  
19 work are expected to contribute to a better understanding on thermo-mechanical behaviours of  
20  
21 MWCNT/epoxy-based composites and would be beneficial toward optimal design of these  
22  
23 composite structures.  
24  
25  
26  
27  
28  
29  
30  
31  
32  
33  
34  
35  
36  
37  
38  
39  
40  
41  
42  
43  
44  
45  
46  
47  
48  
49  
50  
51  
52  
53  
54  
55  
56  
57  
58  
59  
60

## References

- Amir, S., H. BabaAkbar-Zarei and M. Khorasani. 2019. Flexoelectric vibration analysis of nanocomposite sandwich plates. *Mechanics Based Design of Structures and Machines* 1-18. doi: 10.1080/15397734.2019.1624175.
- Anas, S., G.U. Rehman, Z.M. Khan, N. Ul-Haq, M.B. Khan, S. Nauman, M. Shahid and A Nasir. 2014. Influence of MWCNTs as secondary reinforcement material in glass fiber/epoxy composites fabricated using VARTM. *Applied Polymer Composites* 2(1): 17-26.
- Ansari, R., M. K. Hassanzadeh-Aghdam and A. Darvizeh. 2016. Coefficients of thermal expansion of carbon nanotube-reinforced polyimide nanocomposites: A micromechanical analysis. *Proceedings of the Institution of Mechanical Engineers, Part L: Journal of Materials: Design and Applications*, p.1464420716666106. doi:10.1177/1464420716666106.
- Ansari, R., J. Torabi, and M. Faghieh Shojaei. Buckling and vibration analysis of embedded functionally graded carbon nanotube-reinforced composite annular sector plates under thermal loading. *Composites Part B: Engineering* 109: 197-213. doi: 10.1016/j.compositesb.2016.10.050.
- Arefi, M. and A. H. Soltan Arani. 2018. Higher order shear deformation bending results of a magneto-electro-thermoelastic functionally graded nanobeam in thermal, mechanical, electrical, and magnetic environments. *Mechanics Based Design of Structures and Machines*, 46(6): 669-692. doi: 10.1080/15397734.2018.1434002.
- Ayatollahi, M.R., R. Barbaz Isfahani and R. Moghimi Monfared. 2017. Effects of multi-walled carbon nanotube and nanosilica on tensile properties of woven carbon fabric-reinforced epoxy composites fabricated using VARIM. *Journal of Composite Materials*, 51(30): 4177-4188. doi: 10.1177/0021998317699982.
- Barai, P. and G.J. Weng. 2011. A theory of plasticity for carbon nanotube reinforced composites. *International Journal of Plasticity*, 27(4): 539-559. doi: 10.1016/j.ijplas.2010.08.006.
- Bellman, R. and J. Casti. 1971. Differential quadrature and long-term integration. *Journal of Mathematical Analysis and Applications* 34(2): 235-238. doi: 10.1016/0022-247X(71)90110-7.
- Dos Santos, A.S., T.D.O. Leite, C.A. Furtado, C. Welter, L. C. Pardini and G.G. Welter. 2008. Morphology, thermal expansion, and electrical conductivity of multiwalled carbon nanotube/epoxy composites. *Journal of applied polymer science* 108(2): 979-986. doi: 10.1002/app.27614.
- Farzam, A. and B. Hassani. 2018. Thermal and mechanical buckling analysis of FG carbon nanotube reinforced composite plates using modified couple stress theory and isogeometric approach. *Composite Structures* 206:774-790. doi: 10.1016/j.compstruct.2018.08.030.
- Garg, M., S. Sharma and R. Mehta. 2015. Pristine and amino functionalized carbon nanotubes reinforced glass fiber epoxy composites. *Composites Part A: Applied Science and Manufacturing* 76: 92-101. doi: 10.1016/j.compositesa. 2015.05.012.
- Golchi, M., M. Talebitooti and R. Talebitooti. 2019. Thermal buckling and free vibration of FG truncated conical shells with stringer and ring stiffeners using differential quadrature method. *Mechanics Based Design of Structures and Machines* 47(3): 255-282. doi: 10.1080/15397734.2018.1545588.
- Hameed, A., M. Islam, I. Ahmad, N. Mahmood, S. Saeed and H. Javed. 2015. Thermal and mechanical properties of carbon nanotube/epoxy nanocomposites reinforced with pristine and

- functionalized multiwalled carbon nanotubes. *Polymer Composites* 36(10): 1891-1898. doi: 10.1002/pc.23097.
- He, Y., S. Yang, H. Liu, Q. Shao, Q. Chen, C. Lu, Y. Jiang, C. Liu and Z. Guo. 2018. Reinforced carbon fiber laminates with oriented carbon nanotube epoxy nanocomposites: Magnetic field assisted alignment and cryogenic temperature mechanical properties. *Journal of colloid and interface science* 517: 40-51. doi: 10.1016/j.jcis.2018.01.087.
- Kant, T.A.R.U.N. and C.S. Babu. 2000. Thermal buckling analysis of skew fiber-reinforced composite and sandwich plates using shear deformable finite element models. *Composite Structures* 49(1): 77-85. doi: 10.1016/S0263-8223(99)00127-0.
- Kiani, Y., 2017. Thermal buckling of temperature-dependent FG-CNT-reinforced composite skew plates. *Journal of Thermal Stresses* 40(11): 1442-1460. doi: 10.1080/01495739.2017.1336742.
- Kundalwal, S.I. and S.A. Meguid. 2015. Micromechanics modelling of the effective thermoelastic response of nano-tailored composites. *European Journal of Mechanics-A/Solids* 53: 241-253. doi: 10.1016/j.euromechsol.2015.05.008.
- Maghsoudlou, M.A., R. B. Isfahani, S. Saber-Samandari and M. Sadighi. 2019. Effect of interphase, curvature and agglomeration of SWCNTs on mechanical properties of polymer-based nanocomposites: Experimental and numerical investigations. *Composites Part B: Engineering* 175: 107119. doi: 10.1016/j.compositesb.2019.107119.
- Mallick, P.K., 2007. Fiber-reinforced composites: materials, manufacturing, and design. CRC press.
- Manchado, M.L., L. Valentini, J. Biagiotti and J.M. Kenny. 2005. Thermal and mechanical properties of single-walled carbon nanotubes–polypropylene composites prepared by melt processing. *Carbon* 43(7): 1499-1505. doi: 10.1016/j.carbon.2005.01.031.
- Monfared, R.M., M. R. Ayatollahi and R. B. Isfahani. 2018. Synergistic effects of hybrid MWCNT/nanosilica on the tensile and tribological properties of woven carbon fabric epoxy composites. *Theoretical and Applied Fracture Mechanics* 96: 272-284. doi: 10.1016/j.tafmec.2018.05.007.
- Nam, T.H., K. Goto, Y. Shimamura, Y. Inoue and S. Ogihara. 2019. Property improvement of CNT spun yarns and their composites through pressing, stretching and tensioning. *Advanced Composite Materials*: 1-18. doi: 10.1080/09243046.2019.1610586.
- Pötschke, P., A. R. Bhattacharyya, A. Janke and H. Goering. 2003. Melt mixing of polycarbonate/multi-wall carbon nanotube composites. *Composite Interfaces*, 10(4-5): 389-404. doi: 10.1163/156855403771953650.
- Qian, D., E.C. Dickey, R. Andrews and T. Rantell. 2000. Load transfer and deformation mechanisms in carbon nanotube-polystyrene composites. *Applied physics letters* 76(20): 2868-2870. doi: 10.1063/1.126500@apl.2019.APLCLASS2019.issue-1.
- Rafiee, R., 2013. Influence of carbon nanotube waviness on the stiffness reduction of CNT/polymer composites. *Composite Structures* 97: 304-309. doi: 10.1016/j.compstruct.2012.10.028.
- Rahman, M.M., M. Hosur, A.G. Ludwick, S. Zainuddin, A. Kumar, J. Trovillion and S. Jeelani. 2012 a. Thermo-mechanical behavior of epoxy composites modified with reactive polyol diluent and randomly-oriented amino-functionalized multi-walled carbon nanotubes. *Polymer Testing* 31(6): 777-784. doi: 10.1016/j.polymertesting.2012.05.006.
- Rahman, M.M., S. Zainuddin, M. V. Hosur, J. E. Malone, M.B.A. Salam, A. Kumar and S. Jeelani. 2012 b. Improvements in mechanical and thermo-mechanical properties of e-glass/epoxy

- 1  
2  
3 composites using amino functionalized MWCNTs. *Composite Structures*. 94(8): 2397-2406.  
4 doi: 10.1016/j.compstruct.2012.03.014.
- 5 Rahmandoust, M. and M. R. Ayatollahi. 2016. Characterization of carbon nanotube based  
6 composites under consideration of defects, Vol. 1, 12-17. Switzerland: Springer International  
7 Publishing.
- 8 Reddy, J.N., 2004. Mechanics of laminated composite plates and shells: theory and analysis. CRC  
9 press.
- 10 Ren, Y., F. Li, H. M. Cheng and K. Liao. 2003. Tension–tension fatigue behavior of unidirectional  
11 single-walled carbon nanotube reinforced epoxy composite. *Carbon* 41(11): 2177-2179. doi:  
12 10.1016/S0008-6223(03)00248-3.
- 13 Rodríguez-González, J.A. and C. Rubio-González. 2019. Influence of sprayed multi-walled carbon  
14 nanotubes on mode I and mode II interlaminar fracture toughness of carbon fiber/ epoxy  
15 composites. *Advanced Composite Materials*, 28: 19-36. doi: 10.1080/09243046.2018.1458510.
- 16 Salam, M.B.A., M.V. Hosur, S. Zainuddin and S. Jeelani. 2013. Improvement in mechanical and  
17 thermo-mechanical properties of epoxy composite using two different functionalized multi-  
18 walled carbon nanotubes. *Open Journal of Composite Materials* 3(2A): 1-9. doi:  
19 10.4236/ojcm.2013.32A001.
- 20 Sankar, A., S. Natarajan, T. Merzouki and M. Ganapathi. 2017. Nonlinear dynamic thermal  
21 buckling of sandwich spherical and conical shells with CNT reinforced facesheets.  
22 *International Journal of Structural Stability and Dynamics*, 17(09): 1750100. doi:  
23 10.1142/S0219455417501000.
- 24 Şansveren, M.F. and M. Yaman. 2019. The Effect of Carbon Nanofiber on the Dynamic and  
25 Mechanical Properties of Epoxy/Glass Microballoon Syntactic Foam. *Advanced Composite*  
26 *Materials* 1-15. doi: 10.1080/09243046.2019.1610929.
- 27 Schadler, L.S., S.A. Giannaris, and P.M. Ajayan, 1998. Load transfer in carbon nanotube epoxy  
28 composites. *Applied physics letters* 73(26): 3842-3844. doi: 10.1063/1.122911.
- 29 Shahedi, S. and M. Mohammadimehr. 2019. Vibration analysis of rotating fully-bonded and  
30 delaminated sandwich beam with CNTRC face sheets and AL-foam flexible core in thermal  
31 and moisture environments. *Mechanics Based Design of Structures and Machines* 1-31. doi:  
32 10.1080/15397734.2019.1646661.
- 33 Sharma, M. and V. Sharma. 2016. Chemical, mechanical, and thermal expansion properties of a  
34 carbon nanotube-reinforced aluminum nanocomposite. *International Journal of Minerals,*  
35 *Metallurgy, and Materials*, 23(2) 222-233. doi: 10.1007/s12613-016-1230-3.
- 36 Shen, H.S., 2012. Thermal buckling and postbuckling behavior of functionally graded carbon  
37 nanotube-reinforced composite cylindrical shells. *Composites Part B: Engineering* 43(3):  
38 1030-1038. doi: 10.1016/j.compositesb.2011.10.004.
- 39 Shirasu, K., A. Nakamura, G. Yamamoto, T. Ogasawara, Y. Shimamura, Y. Inoue and T. Hashida.  
40 2017. Potential use of CNTs for production of zero thermal expansion coefficient composite  
41 materials: An experimental evaluation of axial thermal expansion coefficient of CNTs using a  
42 combination of thermal expansion and uniaxial tensile tests. *Composites Part A: Applied*  
43 *Science and Manufacturing* 95: 152-160. doi: 10.1016/j.compositesa.2016.12.027.
- 44 Shirasu, K., G. Yamamoto, I. Tamaki, T. Ogasawara, Y. Shimamura, Y. Inoue and T. Hashida.  
45 2015. Negative axial thermal expansion coefficient of carbon nanotubes: Experimental  
46 determination based on measurements of coefficient of thermal expansion for aligned carbon  
47 nanotube reinforced epoxy composites. *Carbon* 95: 904-909. doi:  
48 10.1016/j.carbon.2015.09.026.
- 49  
50  
51  
52  
53  
54  
55  
56  
57  
58  
59  
60

- 1  
2  
3 Shu, C. and B. E. Richards 1992. Application of generalized differential quadrature to solve  
4 two-dimensional incompressible Navier-Stokes equations. *International Journal for*  
5 *Numerical Methods in Fluids*, 15(7): doi: 791-798. 10.1002/flid.1650150704.  
6  
7 Siddiqui, N.A., M.L. Sham, B.Z. Tang, A. Munir and J.K. Kim, 2009. Tensile strength of glass  
8 fibres with carbon nanotube–epoxy nanocomposite coating. *Composites Part A: Applied*  
9 *Science and Manufacturing* 40(10): 1606-1614. doi: 10.1016/j.compositesa.2009.07.005.  
10  
11 Spanos, P.D. and A. Kotsos. 2008. A multiscale Monte Carlo finite element method for  
12 determining mechanical properties of polymer nanocomposites. *Probabilistic Engineering*  
13 *Mechanics* 23(4): 456-470. doi: 10.1016/j.probengmech.2007.09.002.  
14  
15 Torabi, J., R. Ansari and R. Hassani. 2019. Numerical study on the thermal buckling analysis of  
16 CNT-reinforced composite plates with different shapes based on the higher-order shear  
17 deformation theory. *European Journal of Mechanics-A/Solids*, 73: 144-160. doi:  
18 10.1016/j.euromechsol.2018.07.009.  
19  
20 Tung, H.V., 2017. Thermal buckling and postbuckling behavior of functionally graded carbon-  
21 nanotube-reinforced composite plates resting on elastic foundations with tangential-edge  
22 restraints. *Journal of Thermal Stresses* 40(5): 641-663. doi: 10.1080/01495739.2016.1254577.  
23  
24 Yazdi, A.A., 2019. Nonlinear aeroelastic stability analysis of three-phase nano-composite plates.  
25 *Mechanics Based Design of Structures and Machines*: 1-16. doi:  
26 10.1080/15397734.2019.1610436  
27  
28 Zarezadeh, E., V. Hosseini and A. Hadi. 2019. Torsional vibration of functionally graded nano-  
29 rod under magnetic field supported by a generalized torsional foundation based on nonlocal  
30 elasticity theory. *Mechanics Based Design of Structures and Machines*: 1-16. doi:  
31 10.1080/15397734.2019.1642766.  
32  
33 Zhu, J., H. Peng, F. Rodriguez-Macias, J. L. Margrave, V. N. Khabashesku, A. M. Imam, K.  
34 Lozano and E. V. Barrera. 2004. Reinforcing epoxy polymer composites through covalent  
35 integration of functionalized nanotubes. *Advanced Functional Materials* 14(7): 643-648. doi:  
36 10.1002/adfm.200305162.  
37  
38  
39  
40  
41  
42  
43  
44  
45  
46  
47  
48  
49  
50  
51  
52  
53  
54  
55  
56  
57  
58  
59  
60



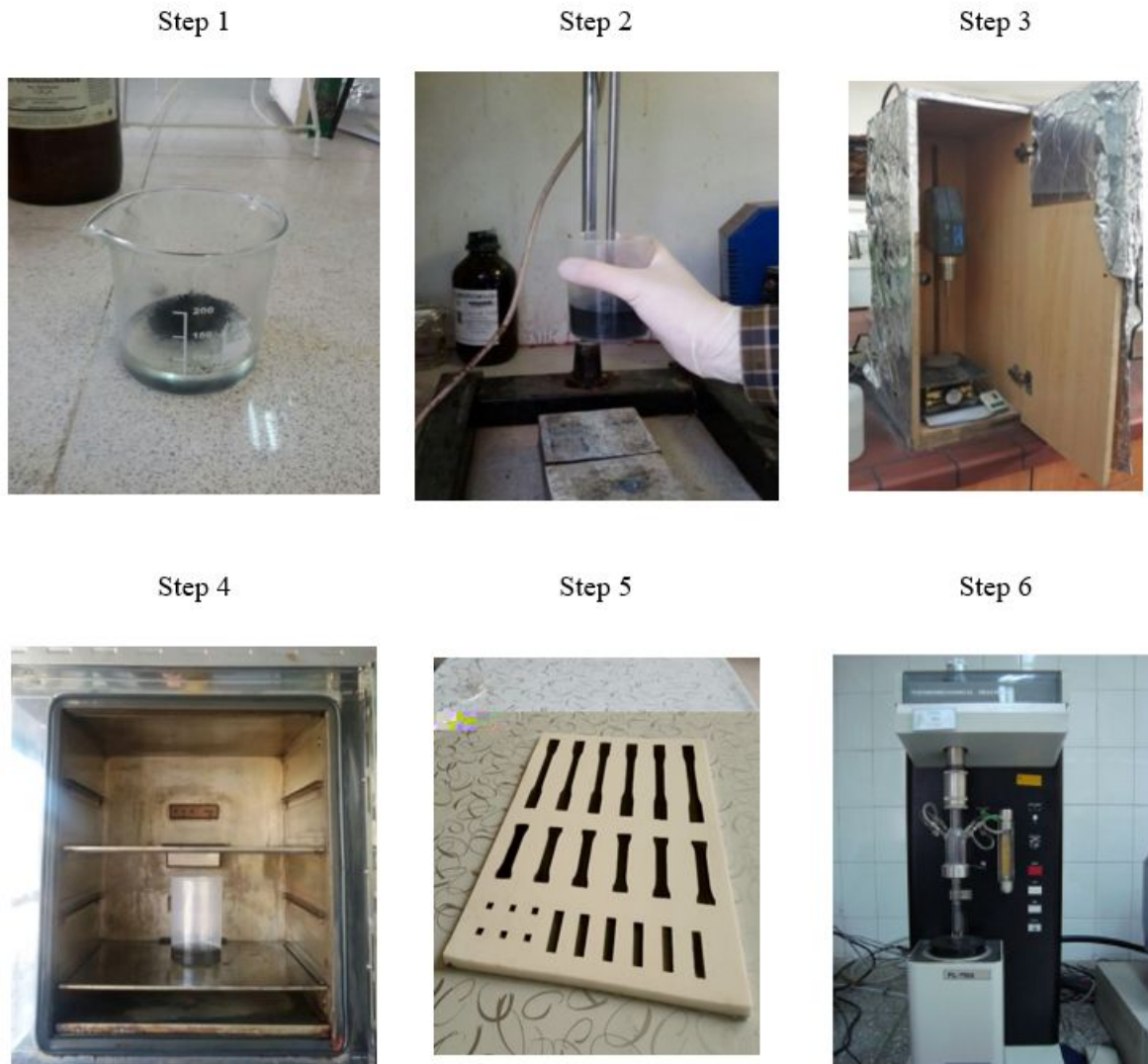
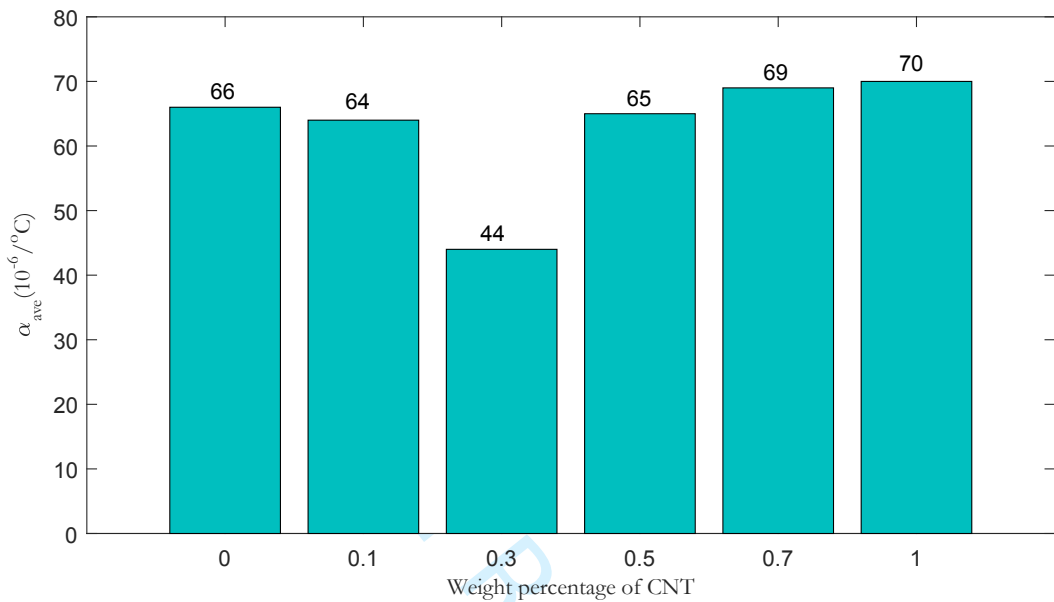
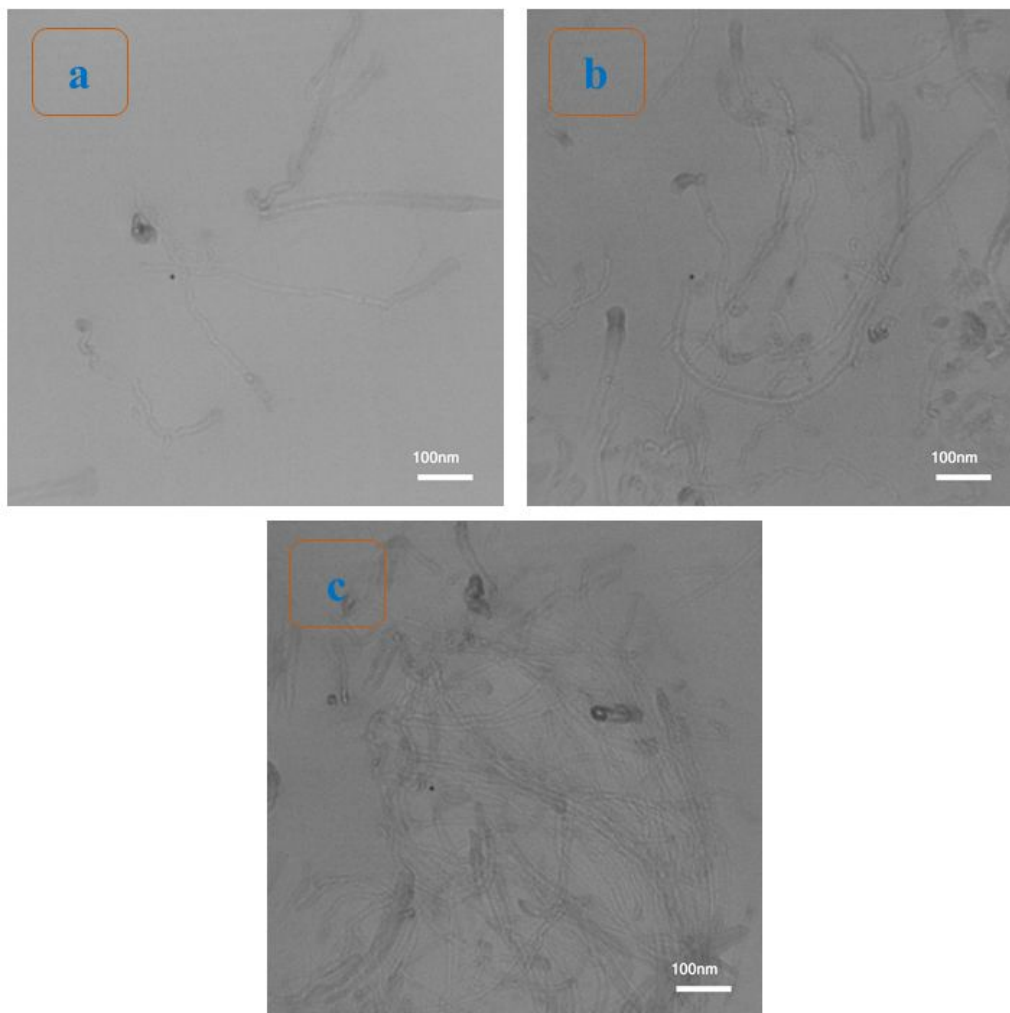


Fig. 1 Preparation of CNT/epoxy samples

1  
2  
3  
4  
5  
6  
7  
8  
9  
10  
11  
12  
13  
14  
15  
16  
17  
18  
19  
20  
21  
22  
23  
24  
25  
26  
27  
28  
29  
30  
31  
32  
33  
34  
35  
36  
37  
38  
39  
40  
41  
42  
43  
44  
45  
46  
47  
48  
49  
50  
51  
52  
53  
54  
55  
56  
57  
58  
59  
60



**Fig. 2** CTE for nanocomposites with different wt.% of MWCNTs.



**Fig. 3** The state of dispersion of MWCNTs in nanocomposite specimens with a) 0.3, b) 0.5 and c) 1 wt. % of nanotubes obtained by TEM.

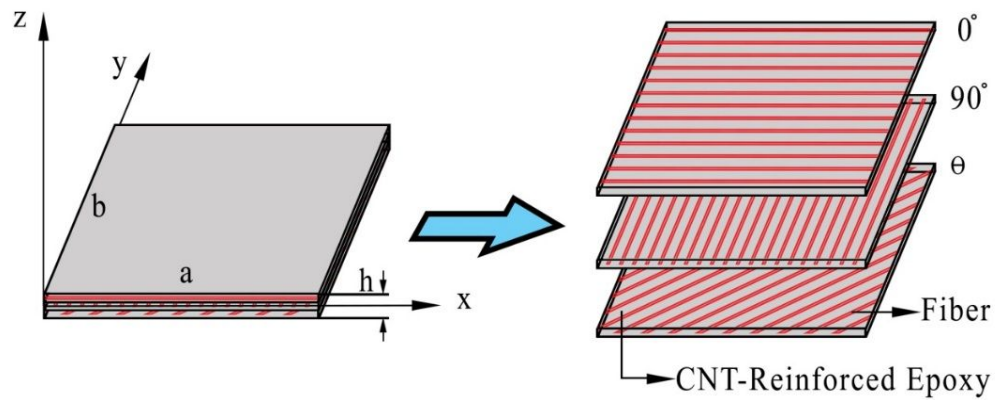


**Fig. 4** Geometry of a rectangular CFRCNT-EP plate

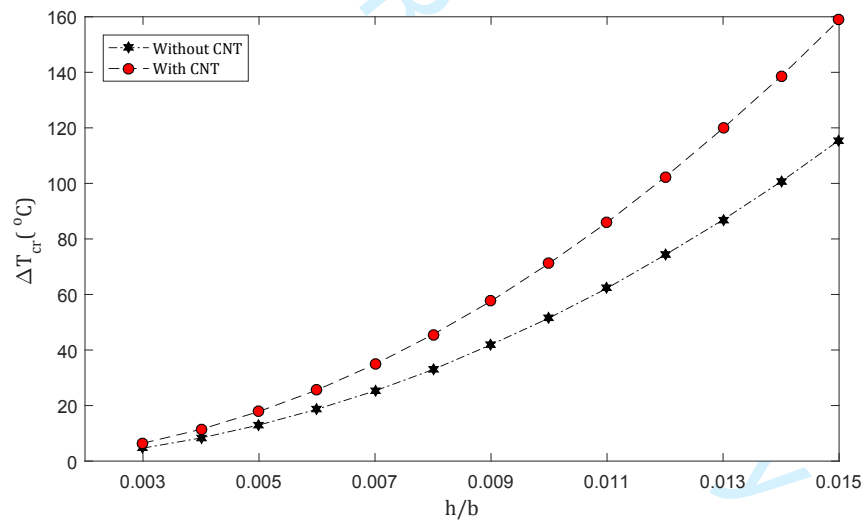


**Fig. 5** The effect of MWCNT on critical buckling temperature of carbon-fiber-reinforced square plates with lamination scheme of  $[30^{\circ} / -45^{\circ} / 90^{\circ}]_s$  and simply supported boundary conditions for different  $h/b$  ratios

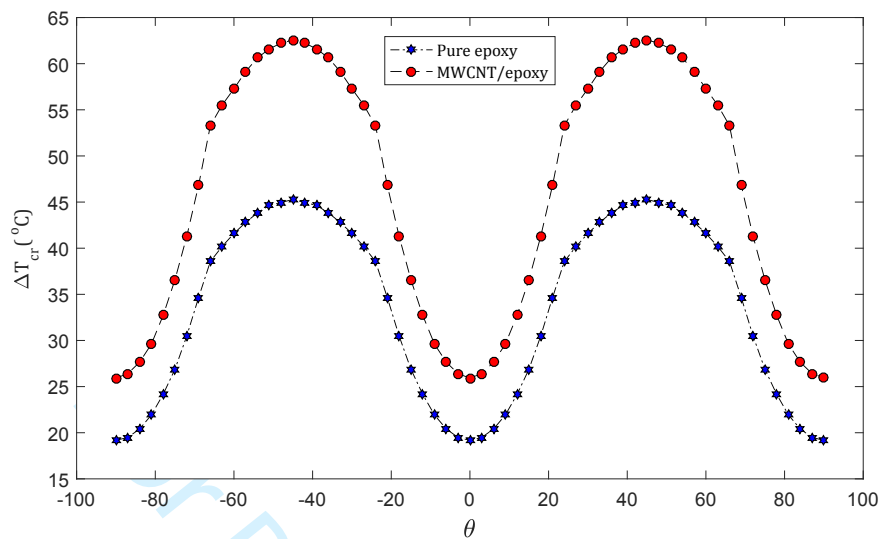


**Fig. 6** The effect of CNTs on critical buckling temperature of  $[\theta/-\theta]_s$  square plates for different lamination scheme ( $h/b=0.01$ )

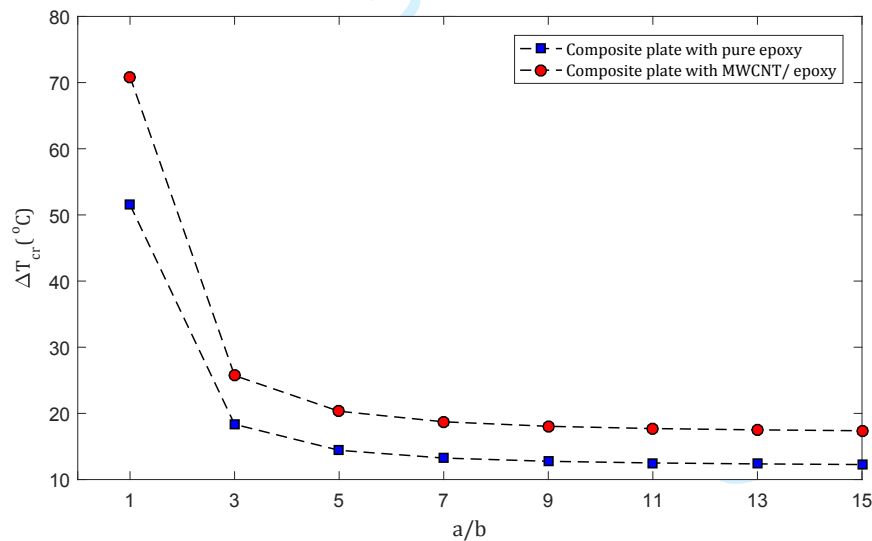


**Fig. 7** The effect of CNTs on critical buckling temperature of rectangular plates with lamination scheme of  $[30^\circ/-45^\circ/90^\circ]_s$  and simply supported boundary conditions against length-to-width ratio ( $h/b=0.01$ )

1  
2  
3  
4  
5  
6  
7  
8  
9  
10  
11  
12  
13  
14  
15  
16  
17  
18  
19  
20  
21  
22  
23  
24  
25  
26  
27  
28  
29  
30  
31  
32  
33  
34  
35  
36  
37  
38  
39  
40  
41  
42  
43  
44  
45  
46  
47  
48  
49  
50  
51  
52  
53  
54  
55  
56  
57  
58  
59  
60

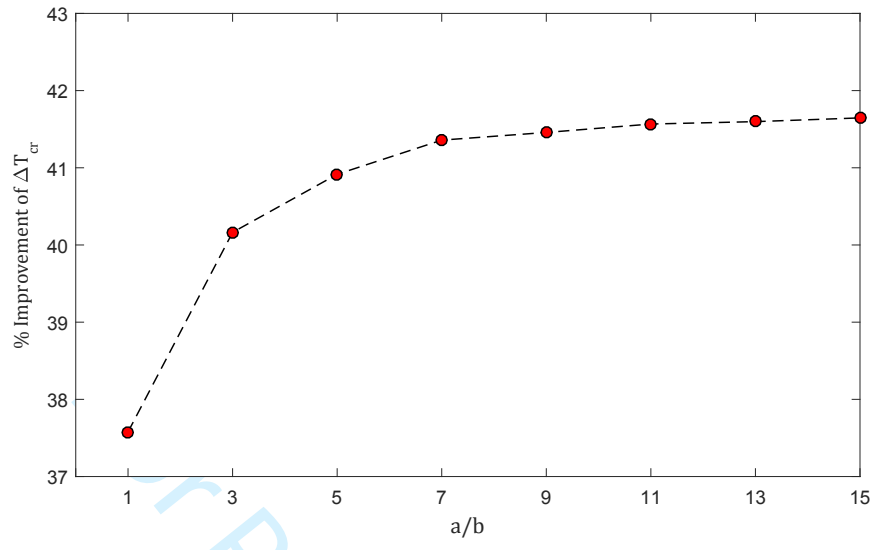


**Fig. 8** The amount of increase of buckling temperature of simply supported  $[30^{\circ} / -45^{\circ} / 90^{\circ}]_s$  rectangular plates by adding CNTs into the polymer matrix ( $h/b=0.01$ )

**Table 1.** Thermal expansion coefficient from the present TMA test and manufacturer's date sheet

TMA test	Thermal Expansion Coefficient ( $\alpha \times 10^{-6} \text{ }^{\circ}\text{C}^{-1}$ )			
	manufacturer's date sheet			TMA test
	$25^{\circ}\text{C}/7d$	$50^{\circ}\text{C}/15h$	$80^{\circ}\text{C}/8h$	
20-50	97	-	-	-
20-90	-	71	-	-
20-120	-	-	71	66

**Table 2.** Mean value of CTE ( $\times 10^6 / ^{\circ}\text{C}$ ) for experimental tests against different CNT weight percentages

	wt% of CNTs					
	0	0.1	0.3	0.5	0.7	1
Mean Value of CTE	66	64	44	65	69	70

**Table 3.** Material properties of the pure epoxy and CNT/epoxy nanocomposite adopted from different methods.

Property	Unit	Pure Epoxy		CNT-Reinforced Epoxy	
		Value	Method	Value	Method
Young's Modulus	<i>GPa</i>	3.10	Data Sheet	3.38	Theoretical Model
CTE	$10^{-6} / ^{\circ}\text{C}$	66	Experiment	44	Experiment
Poisson's Ratio	-	0.35	Data Sheet	0.35	Assumption

**Table 4.** Material properties of the carbon fibers

Property	Unit	Value
$E_1$	<i>GPa</i>	225
$E_2$	<i>GPa</i>	15
$G_{12}$	<i>GPa</i>	15
$\nu_{12}$	-	0.2
$\alpha_1$	$10^{-6} / ^\circ\text{C}$	-0.5
$\alpha_2$	$10^{-6} / ^\circ\text{C}$	15

**Table 5.** Material properties of CFREP and CFRCNTEP composites.

Property	Unit	CFREP Composite	CFRCNTEP Composite	Improvement (%)
$E_1$	<i>GPa</i>	136.24	136.25	0.08
$E_2$	<i>GPa</i>	6.59	7.02	6.52
$G_{12}$	<i>GPa</i>	2.57	2.78	8.17
$\nu_{12}$	-	0.35	0.35	0
$\alpha_1$	$10^{-6} / ^\circ\text{C}$	0.105	-0.059	156.19
$\alpha_2$	$10^{-6} / ^\circ\text{C}$	44.553	32.716	26.57

**Table 6.** Convergence and accuracy of the critical buckling temperature parameter ( $\lambda_T = 100\alpha_0\Delta T_{cr}$ ) of cross-ply  $[0^\circ/90^\circ]_s$  rectangular plates for different boundary conditions

$$(a/b = 1, h/b = 0.01, \alpha_0 = 10^{-6} 1/^\circ\text{C}).$$

BCs	$N_x = N_y$				Kant and Babu 2000
	9	11	13	17	
SSSS	0.0992	0.0996	0.0996	0.0996	0.0997
CCCC	0.3355	0.3354	0.3354	0.3354	0.3352



**Table 7.** The effect of MWCNT on critical buckling temperature of carbon-fiber-reinforced square plates with lamination scheme of  $[30^{\circ}/-45^{\circ}/90^{\circ}]_s$  and simply supported boundary conditions for different  $h/b$  ratios

$h/b$	Pure Epoxy Matrix	MWCNT/Epoxy Matrix	Improvement (%)
0.003	4.68	6.44	37.61
0.004	8.32	11.44	37.50
0.005	12.99	17.87	37.57
0.006	18.69	25.60	36.97
0.007	25.28	34.88	37.97
0.008	32.96	45.60	38.35
0.009	41.92	57.60	37.40
0.010	51.52	71.18	38.16
0.011	62.24	85.92	38.04
0.012	74.24	102.24	37.72
0.013	86.88	119.84	37.93
0.014	100.64	138.56	37.68
0.015	115.52	158.88	37.53

**Table 8.** The influence of CNTs on critical buckling temperature of  $[30^{\circ}/-45^{\circ}/90^{\circ}]_s$  plates for different boundary conditions ( $a/b = 1, h/b = 0.01$ ).

Boundary Conditions	Epoxy Matrix	MWCNT/Epoxy Matrix	Improvement (%)
<i>SSSS</i>	51.52	70.88	37.58
<i>SCSC</i>	72.96	100.96	38.38
<i>CCCC</i>	116.66	160.64	37.70